INSTITUTE OF PHYSICS PUBLISHING CLASSICAL AND QUANTUM GRAVITY

Class. Quantum Grav. **20** (2003) S109–S116 PII: S0264-9381(03)55737-9

ST-7 gravitational reference sensor: analysis of magnetic noise sources

John Hanson[1], G Mac Keiser[2], Saps Buchman[2], Robert Byer[2], Dave Lauben[2], Daniel DeBra[2], Scott Williams[2], Dale Gill[2], Ben Shelef[3] and Gad Shelef[3]

[1] CrossTrac Engineering, 437G Costa Mesa Terrace, Sunnyvale, CA 94087, USA
[2] Hansen Experimental Physics Laboratory, Stanford University, CA, USA
[3] Gizmonics, Inc.

E-mail: hanson@netwizards.net

Received 7 November 2002, in final form 25 February 2003
Published 28 April 2003
Online at stacks.iop.org/CQG/20/S109

Abstract

A next generation gravitational reference sensor is being developed by Stanford University for the disturbance reduction system (DRS). The DRS will demonstrate the technology required for future gravity missions, including the planned LISA gravitational-wave observatory. The GRS consists of a freely floating test mass, a housing, sensing electrodes and associated electronics. Position measurements from the GRS are used to fly the spacecraft in a drag-free trajectory, where spacecraft position will be continuously adjusted to stay centred about the test mass, essentially flying in formation with it. Any departure of the test mass from a gravitational trajectory is characterized as acceleration noise, resulting from unwanted forces acting on the test mass. The GRS will have an inherent acceleration noise level more than four orders of magnitude lower than previously demonstrated in space. To achieve such a high level of performance, the interaction of the magnetized test mass with the magnetic fields produced by the spacecraft must be considered carefully. It is shown that a new noise source due to the interaction of the time-varying magnetic field gradient and the permanent dipole of the test mass must be added to the noise analysis. A simple current loop model shows that the design of the spacecraft and instrument electronics must be done with attention to the magnetic noise produced.

PACS number: 04.80.Nn

(Some figures in this article are in colour only in the electronic version)

1. Introduction

In the next decade, several new missions will require the development of a new generation of gravitational reference sensor (GRS). These include the Laser Interferometer Space Antenna

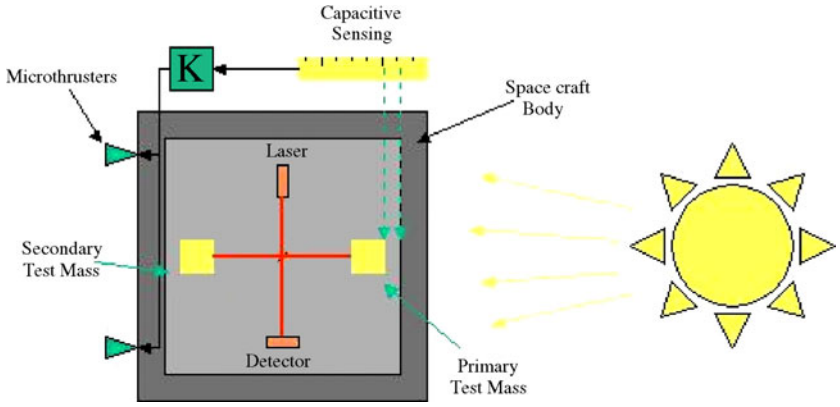

Figure 1. The DRS mission concept.

(LISA, which will search for low-frequency gravitational waves), EX-5 (mapping of time-varying earth gravitational fields) and LIRE (test of general relativity). All of these missions utilize drag-free satellites and an improvement in the performance of existing gravitational sensors of several orders of magnitude in both residual acceleration and low frequency coverage is necessary.

The GRS is the enabling technology for drag-free satellites. First flown in 1973 as TRIAD-1 [1], the goal of drag-free satellites is to fly in a perfectly gravitational trajectory. This is achieved by building a spacecraft around a test mass, sensing the position of the spacecraft relative to the test mass and firing thrusters to control the position of the spacecraft such that the test mass 'floats' inside its housing, unaffected by the spacecraft or external disturbances. Because the spacecraft is following the trajectory of the undisturbed test mass, it is also flying a drag-free trajectory. The key performance metric for a gravitational reference sensor is the *residual acceleration* in the frequency band of interest. These extraneous accelerations come from several sources, including mass attraction between the test mass and the spacecraft, residual gas pressure in the housing, interactions between the proof mass and magnetic fields and forces used to constrain the test mass in non-sensitive degrees of freedom.

The disturbance reduction system (DRS) mission, which will fly on the SMART-2 spacecraft in late 2006, has two key objectives [7]: to demonstrate the operation of a gravitational reference sensor with residual acceleration levels in the sensitive axis at or below 3×10^{-14} m s^{-2} Hz$^{-1/2}$ between 1 mHz and 10 mHz; and to demonstrate a system for sensing the position of the proof mass relative to the housing with an accuracy of 3×10^{-9} m Hz$^{-1/2}$ in the same band.

As shown in figure 1, the residual acceleration acting on the GRS will be measured by flying two GRSs on the same spacecraft. The positions of the two test masses will be measured relative to one another in the sensitive direction with an interferometer mounted between them. The primary test mass serves as a drag-free reference. Its position relative to the housing is measured capacitively and a set of microthrusters keep the spacecraft centred about it. By properly controlling the spacecraft rotation, the second test mass can be unconstrained in its two transverse degrees of freedom as well. However, the sensitive axis of the secondary test mass will not be drag free. Low-frequency forces (below the measurement band) are the result of spacecraft mass attraction, and electrostatic and magnetostatic fields, and will cause the secondary test mass to drift in the sensitive direction if it is not constrained. On DRS,

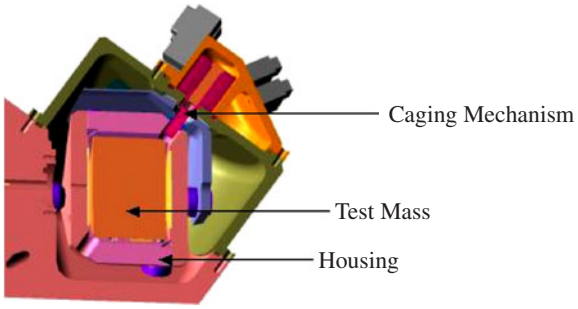

Figure 2. The gravitational reference sensor.

the motion of the secondary test mass is controlled below 1 mHz by forcing the test mass electrostatically.

The GRS being developed at Stanford University is shown in figure 2. Key to its operation is a 4 cm Au–Pt cube. This proof mass is placed inside a ceramic housing made from beryllia to minimize temperature gradients. The gap between any housing surface and the proof mass is 2 mm. Fourteen gold-plated electrodes, deposited on the housing walls, are used to measure the position of the proof mass capacitively and exert electrostatic forces on it to control its position, as necessary. A pneumatic caging mechanism holds the mass in place to prevent damaging its highly polished surface on launch. The charge of the test mass is controlled with an ultraviolet charge-management system. Not shown in the figure are the analogue electronics, which measure and control the proof mass position and the digital electronics, consisting primarily of a flight processor and input/output electronics.

The GRS must demonstrate residual acceleration levels in the sensitive axis at or below 3×10^{-14} m s^{-2} Hz$^{-1/2}$ between 1 mHz and 10 mHz. The performance of similar GRS designs have been analysed by Vitale [3] and Schumaker [4]. Recent measurements of the magnetic properties of 70/30 Au–Pt have been made by Gill and Mester [5]. While they confirm the low magnetic susceptibility of the material, the samples (each approximately 4 g in mass) also had a small permanent magnetic dipole of the order of 8×10^{-8} A m^2 kg^{-1}. At this time it is not clear whether the measurement is due to ferromagnetic impurities that are volume (and hence mass) dependent, impurities on the surface or due to the noise floor of the measurement apparatus. Scaling the permanent magnetic dipole by the relative masses of the test sample and the proof mass, a conservative estimate of the remanent moment of the 1.3 kg test mass is shown to be 10^{-7} A m^2. This introduces a new noise source that must be considered in the design of the GRS. In fact, in order to keep the residual acceleration due to remanent moment interaction to an acceptable level, one must either carefully control the magnetic cleanliness of the spacecraft and instruments, or shield the sensor from external magnetic fields with a high-permeability magnetic shield, a solution that is not considered here.

Several different types of noise contribute to the GRS total residual acceleration budget, the current version of which is shown in table 1 (for a more complete discussion of these noise sources, see Vitale [3], Schumaker [4] and Hanson [6]). These can be divided into those that are time invariant, but a function of proof mass position (stiffness terms) and those that are time variant, but independent of position (direct terms). The stiffness terms are due to electrostatic field gradients, mass attraction gradients and second-order derivatives of the magnetic field, and effectively couple spacecraft jitter into proof mass acceleration (hence, spacecraft coupled force). Direct force terms include effects such as variations in electrode potential (back action),

Table 1. Gravitational reference sensor noise budget.

Noise source	Requirement (m s^{-2} $Hz^{-1/2}$)
Requirement	2.5×10^{-14}
Electrostatic suspension—back action	1.0×10^{-14}
Dielectric effect	0.02×10^{-14}
Lorentz force	0.4×10^{-14}
Proof mass magnetic susceptibility, χ	0.3×10^{-14}
Proof mass remanent moment	0.6×10^{-14}
Radiometer effect	0.25×10^{-14}
Housing temperature gradient	0.25×10^{-14}
Interferometer laser power variations	0.1×10^{-14}
Residual gas pressure damping	0.15×10^{-14}
Time-varying mass attraction gradients	0.5×10^{-14}
Coupled control force	1.0×10^{-14}
Spacecraft coupled force	1.8×10^{-14}
Total residual acceleration	2.5×10^{-14}

interactions between the charged test mass and the interplanetary magnetic field (Lorentz force), interactions between the magnetized proof mass and its surroundings and temperature effects such as the radiometer effect and housing temperature gradients. In addition, changes in the interferometer light pressure will introduce an unwanted acceleration of the proof mass.

2. Acceleration due to magnetic field interactions

Because recent measurements of the magnetic properties of Au–Pt alloys indicate that a permanent magnetic dipole will be present in the test mass, these magnetic interactions require more detailed analysis. The acceleration of an object with a magnetic dipole[4] in a magnetic field will have a time-dependent component and a position-dependent component:

$$\vec{f} = \frac{1}{m}\nabla(\vec{M}\cdot\vec{B}) + \frac{1}{m}\nabla[\nabla(\vec{M}\cdot\vec{B})]\cdot\vec{n}_{sc}. \tag{1}$$

The first term contains the constant force and the time-varying force, while the second term is due to the interaction of the spacecraft motion with a magnetic field that changes with position in the GRS housing. This relates the acceleration to motion in translation.

Preliminary measurements of the magnetic properties of Au–Pt alloys suggest that their magnetic dipole (M) consists of a remanent moment term and an induced moment term:

$$\vec{M} = \vec{M}_r + \frac{\chi\cdot V}{\mu_0}\vec{B}. \tag{2}$$

The magnetic field can be partitioned into a constant field B_0 and a time-varying field $b(t)$:

$$\vec{B} = \vec{B}_0 + \vec{b}(t). \tag{3}$$

Combining these three equations and collecting terms, it can be shown that the acceleration on the test mass is a combination of the steady force (f_{dc}), the force due to magnetic susceptibility (f_x), the force due to remanent moment (f_r) and the stiffness term (K_m):

[4] Jackson John David 1999 *Classical Electrodynamics* (New York: Wiley) p 189.

Constant term $$\vec{f}_{dc} = \frac{1}{m}[\nabla \vec{B}_0]\left(\vec{M}_r + 2\frac{\chi V}{\mu_0}\vec{B}_0\right) \tag{4a}$$

Magnetic susceptibility term $$\vec{f}_x = 2\frac{\chi}{\rho\mu_0}\{[\nabla \vec{B}_0]\vec{b}(t) + [\nabla \vec{b}(t)](\vec{B}_0 + \vec{b}(t))\} \tag{4b}$$

Remanent moment term $$\vec{f}_r = [\nabla \vec{b}(t)]\frac{\vec{M}_r}{m} \tag{4c}$$

Magnetic stiffness $$k_m = \frac{1}{m}\nabla[\nabla(\vec{M}\cdot\vec{B})]. \tag{4d}$$

The new noise term that has been identified is due to the interaction between the permanently magnetized test mass and the time-varying magnetic field gradient. This introduces an additional requirement on the spacecraft. The time change in the gradient must be sufficiently small to make this noise term comparable to other noise terms in the budget.

The terms of the stiffness matrix (k_m) can be determined by considering the force in each axis in turn. Thus, the gradient of the force in the x direction yields the first row of k_m, and so on. Of primary concern is the coupling of any spacecraft motion into an acceleration in the sensitive axis (x-axis). The stiffness terms that couple motion into the sensitive axis are related to the gradient of the force in the sensitive direction:

$$[k_{xx} \quad k_{xy} \quad k_{xz}] = (\nabla f_x)^T. \tag{5}$$

Substituting the constant force term above into this stiffness equation, the gradient of this force is

$$\nabla f_x = \frac{1}{m}\nabla\left\{\begin{bmatrix}\frac{\partial B_x}{\partial x} & \frac{\partial B_y}{\partial x} & \frac{\partial B_z}{\partial x}\end{bmatrix}\vec{M}_r\right\} + 2\frac{\chi}{\rho\mu_0}\nabla\left\{\begin{bmatrix}\frac{\partial B_x}{\partial x} & \frac{\partial B_y}{\partial x} & \frac{\partial B_z}{\partial x}\end{bmatrix}\vec{B}\right\} \tag{6}$$

$$\nabla f_x = \begin{bmatrix}\frac{\partial^2 B_x}{\partial x^2} & \frac{\partial^2 B_y}{\partial x^2} & \frac{\partial^2 B_z}{\partial x^2} \\ \frac{\partial^2 B_x}{\partial x\partial y} & \frac{\partial^2 B_y}{\partial x\partial y} & \frac{\partial^2 B_z}{\partial x\partial y} \\ \frac{\partial^2 B_x}{\partial x\partial z} & \frac{\partial^2 B_y}{\partial x\partial z} & \frac{\partial^2 B_z}{\partial x\partial z}\end{bmatrix}\left\{\frac{\vec{M}_r}{m} + 2\frac{\chi}{\rho\mu_0}\vec{B}\right\} + 2\frac{\chi}{\rho\mu_0}[\nabla\vec{B}]\begin{bmatrix}\frac{\partial B_x}{\partial x} & \frac{\partial B_y}{\partial x} & \frac{\partial B_z}{\partial x}\end{bmatrix}^T. \tag{7}$$

This stiffness term puts upper bounds on the spatial derivatives of the magnetic field. This bound applies to all magnetic field components since the orientation of the remanent moment in the test mass and the direction of the nominal magnetic field direction are unknown. The GRS magnetic field requirements and residual accelerations due to magnetic susceptibility and remanent moment are summarized in table 2.

3. Sources of magnetic fields

Having established the requirements for the magnetic field at the test mass location, we consider the potential sources of magnetic field. These sources fall into three general categories: the natural environment, permanent magnets on the spacecraft and spacecraft and instrument electrical circuits. The local solar magnetic field is about four orders of magnitude weaker than the allowable spacecraft magnetic field and is further reduced by the presence of electrostatic shielding on the GRS. Permanent magnetic dipoles associated with the laser, dc–dc converters

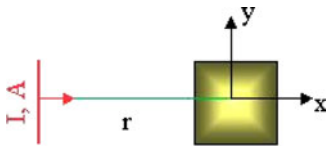

Figure 3. A spacecraft magnetic dipole example.

Table 2. Magnetic field requirements.

Item	Symbol	Requirement	Units
Acceleration—magnetic susceptibility		3×10^{-15}	m s^{-2} Hz$^{-1/2}$
Acceleration—remanent moment		6×10^{-15}	m s^{-2} Hz$^{-1/2}$
Magnetic susceptibility	χ	4×10^{-6}	(SI)
Proof mass density	ρ	2×10^{4}	kg m^{-3}
Steady magnetic field	B_0	1×10^{-5}	T
Time-varying magnetic field	$b(t)$	1×10^{-6}	T Hz$^{-1/2}$
Steady magnetic field gradient	$\mathrm{d}B_0/\mathrm{d}z$	6×10^{-6}	T m^{-1}
Time-varying magnetic field gradient	$\mathrm{d}b(t)/\mathrm{d}z$	4×10^{-8}	T m^{-1} Hz$^{-1/2}$
Second gradient of magnetic field	$\mathrm{d}^2B/\mathrm{d}z^2$	0.3	T m^{-2}
Remanent moment	M_r	1.3×10^{-7}	A m^2
Mass of test mass	m	1.3	kg

and latching valves can be modelled as magnetic dipoles distributed throughout the spacecraft. Temperature fluctuations will cause the positions and orientations of the dipoles relative to the test mass to change with time, contributing to the time-varying magnetic field and the time-varying magnetic field gradient. Current loops in the electronics (e.g., traces on a board or through harnesses) will create magnetic dipoles that behave in a similar fashion, contributing a steady magnetic field, gradient terms and time-varying terms. In addition, changes in the current flowing through such a loop will contribute additional time varying magnetic field noise and time-varying magnetic field gradient noise.

As an example, the dipole created by a single current loop is used to demonstrate the sensitivity of the GRS to the design of the electronics. The contribution of permanent magnets can be considered in a similar fashion.

Consider the planer case shown in figure 3 where a magnetic dipole is co-aligned with the test mass sensitive axis, some distance (r) away. The components of the magnetic field in the x and y directions are

$$B_x = \frac{\mu_0}{4\pi}\frac{3x^2 - r^2}{r^5}[AI] \qquad B_y = \frac{\mu_0}{4\pi}\frac{xy}{r^5}[AI].$$

It can be shown that the contributions of the current loop to the magnetic field terms of interest are

$$\frac{\partial B_x}{\partial x} = \frac{-3}{r}B_x \qquad b_x(t) = -3B_x\frac{\Delta r}{r} + B_x\frac{\Delta I}{I} + B_x\frac{\Delta A}{A}$$

$$\frac{\partial^2 B_x}{\partial x^2} = \frac{12}{r^2}B_x \qquad \frac{\partial b_x(t)}{\partial x} = \left(\frac{\partial B_x}{\partial x}\right)\frac{b_x(t)}{B_x} + 3B_x\frac{\Delta r}{r^2}.$$

The magnetic field characteristics of a typical current loop (i.e., magnetic dipole) are shown in figure 4. In all cases, a nominal dipole of 0.1 A m^2 is assumed. This could represent a single large dipole, or the sum of a large number of smaller dipoles on the spacecraft.

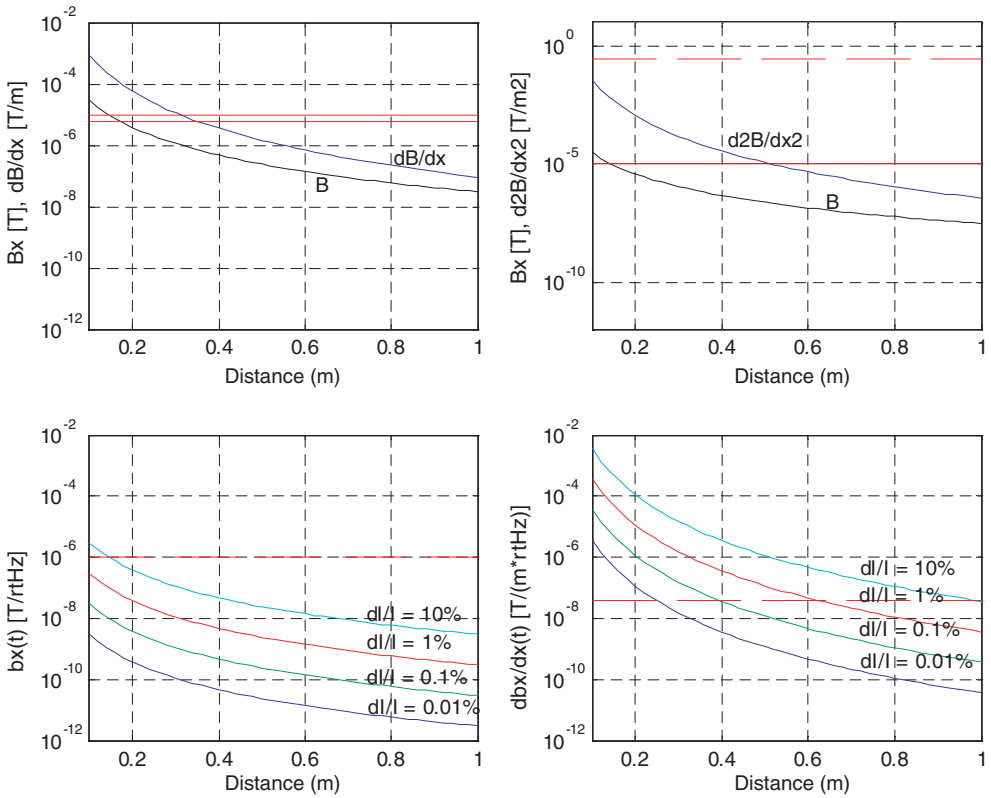

Figure 4. Magnetic field characteristics due to the current loop.

In either case, it is clear that in order to meet the requirement for the time-varying magnetic field gradient, care must be taken in designing all the electrical systems and their placements relative to the GRS proof masses.

4. Summary

The gravitational reference sensor being developed by Stanford University will have a residual acceleration in the sensitive axis at or below 3×10^{-14} m s^{-2} Hz$^{-1/2}$ between 1 mHz and 10 mHz, and will demonstrate a system for sensing the position of the proof mass with an accuracy of 3×10^{-9} m Hz$^{-1/2}$ in the same band. Recent measurements of the magnetic properties of Au–Pt alloys have added to the understanding of GRS performance. Interactions between the permanently magnetized test mass and the magnetic fields generated on the spacecraft make significant contributions to the noise. While improved processing may reduce the size of the remanent moment, a careful design of the spacecraft electrical systems is still the key to mission success.

Acknowledgment

This work was performed under JPL contract no 1232133 as part of the ST-7 Drag Reduction System, a New Millennium Program.

References

[1] Space-Dept A P L and Guidance Control Laboratory 1974 A satellite freed of all but gravitational forces: TRIAD I *J. Spacecraft* **11** 637–44

[2] Keiser G M, Buchman S, Bencze W and DeBra D B 1998 The expected performance of gravity probe B electrically suspended gyroscopes as differential accelerometers *2nd Int. LISA Symp. and the Detection and Observation of Gravitational Waves in Space*

[3] Bortoluzzi D *et al* 2003 The Lisa Technology Package on board SMART-2 *Proc. 4th Int. LISA Symp. (Pennsylvania, July 2002) Class. Quant. Grav.* **20** S89

[4] Schumaker B 2003 Disturbance reduction requirements for LISA *Proc. 4th Int. LISA Symp. (Pennsylvania, July 2002) Class. Quant. Grav.* **20** S239

[5] Gill D *et al* 2002 Test mass material selection and fabrication processes for the ST-7 gravitational reference sensor *34th COSPAR Scientific Assembly (Houston, TX, Oct. 2002)*

[6] Hanson J *et al* 2002 The disturbance reduction system: testing technology for drag free operation *SPIE Astronomical Telescopes and Instrumentation (Hawaii, Aug. 2002)*

[7] Vitale S *et al* 2002 LISA and its in-flight test precursor SMART-2 *Nucl. Phys.* B *Proc. Suppl.* **110** 209